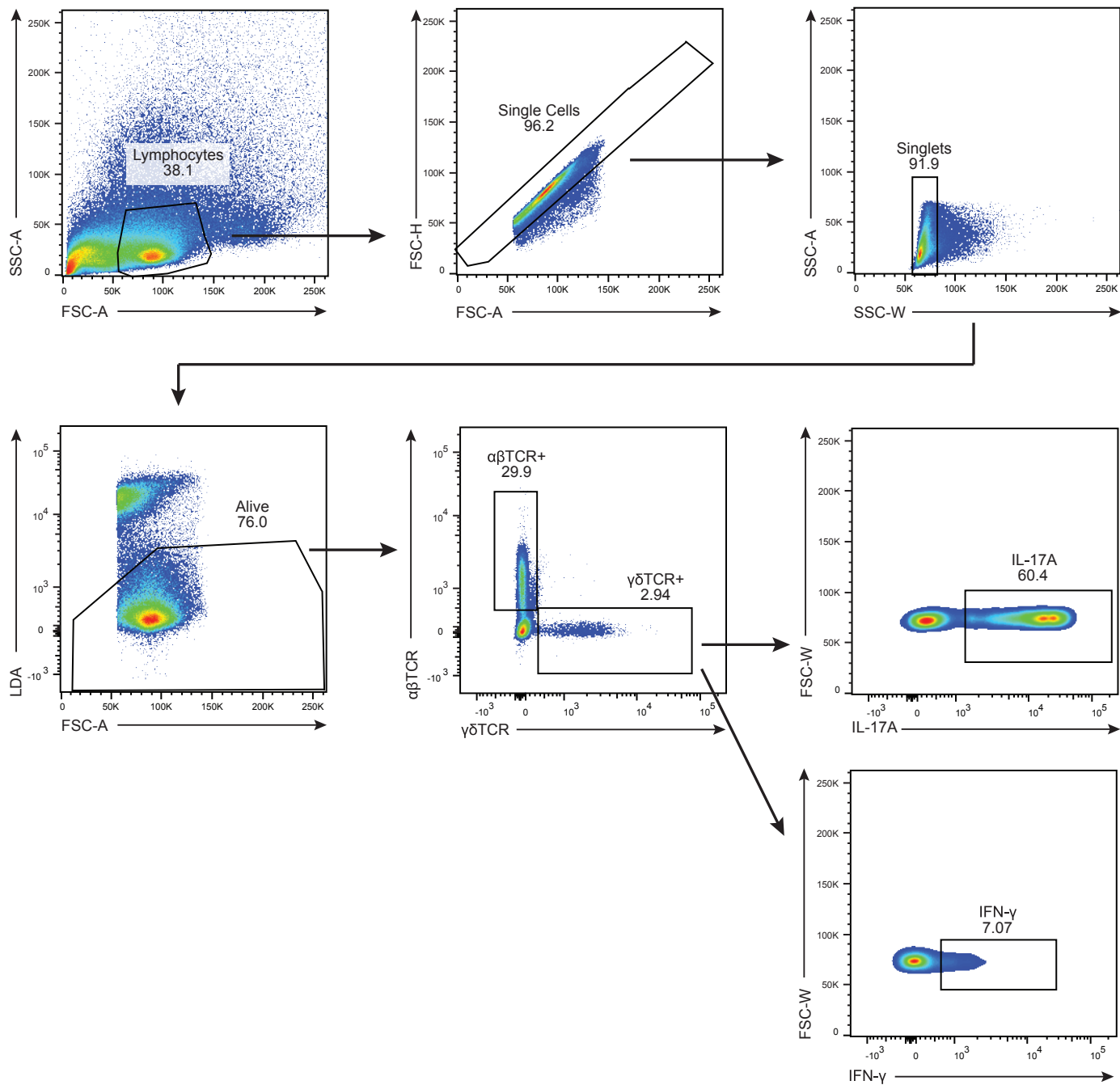
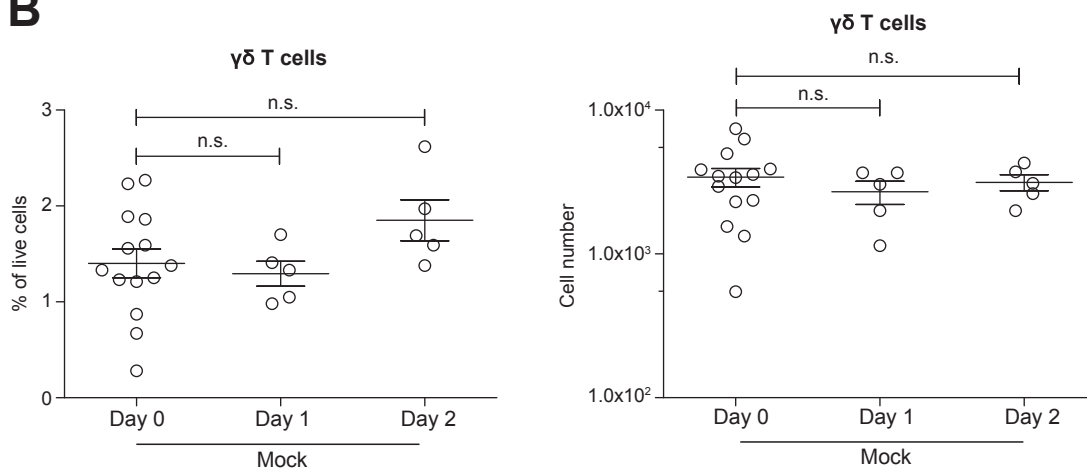


A**B****Figure S1**

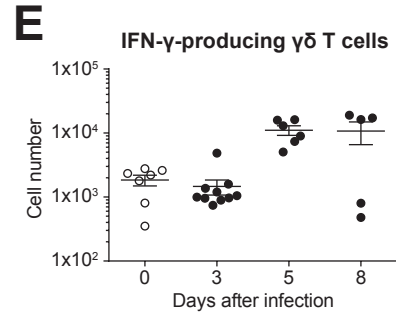
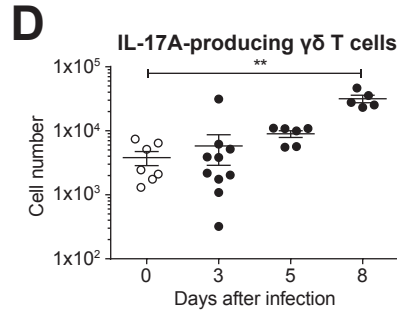
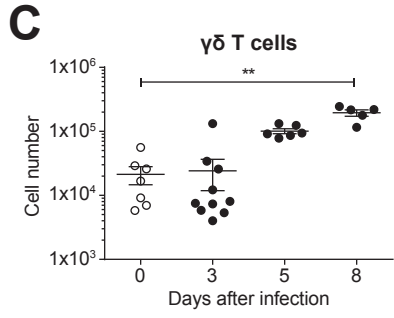
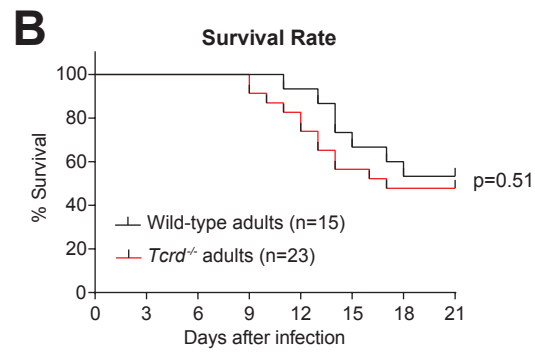
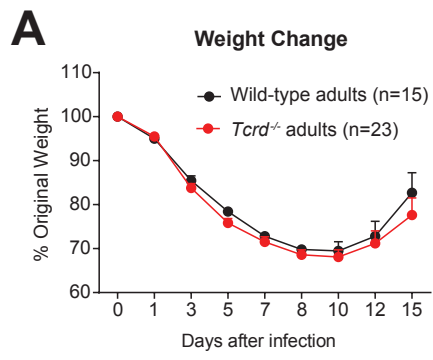


Figure S2

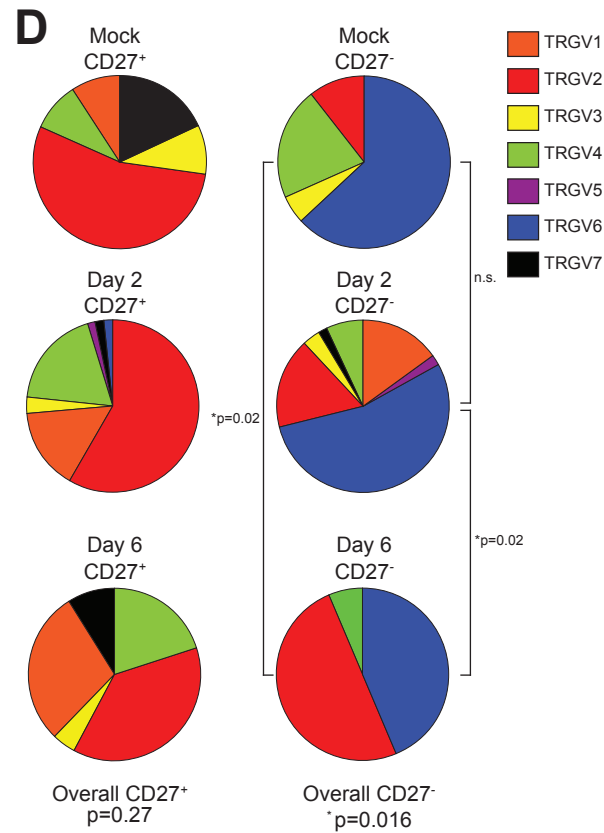
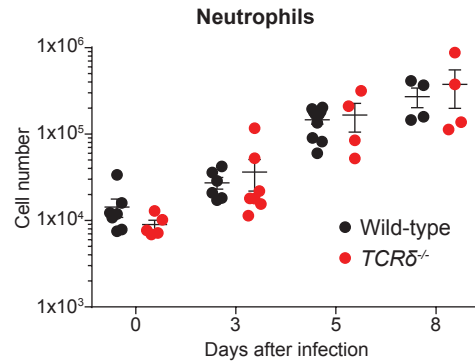
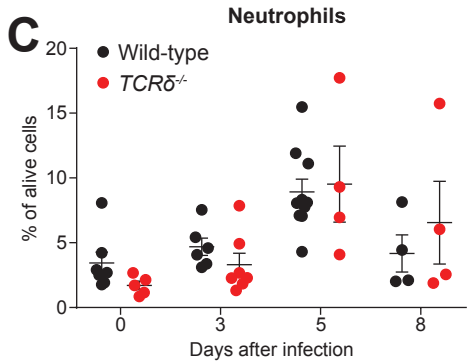
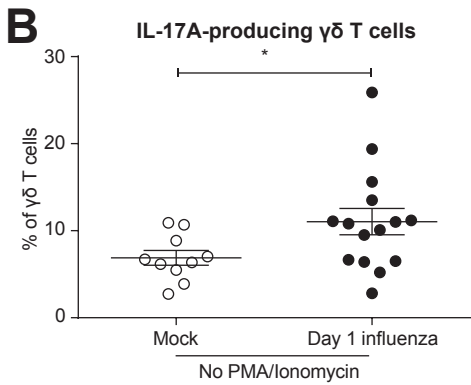
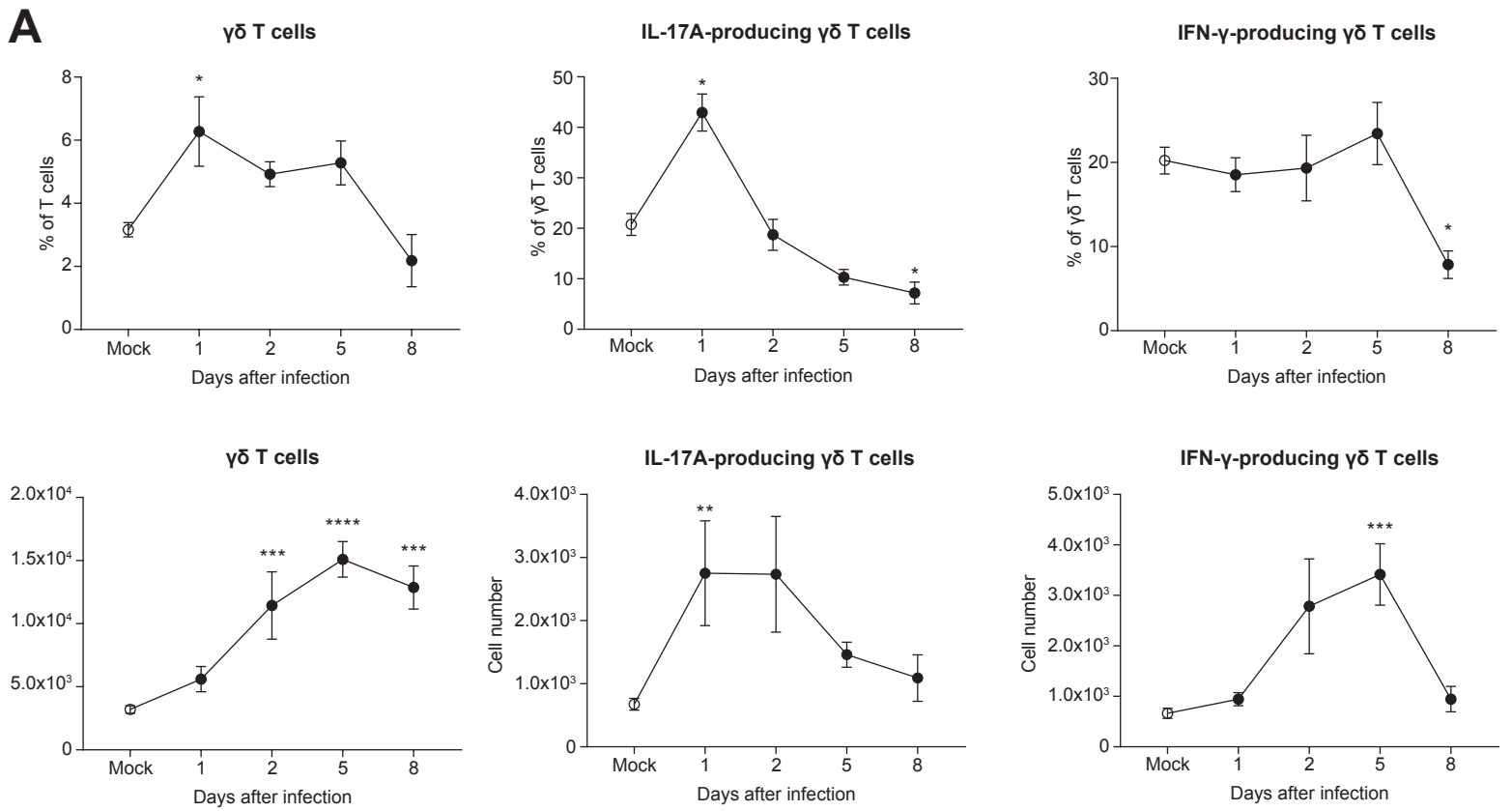


Figure S3

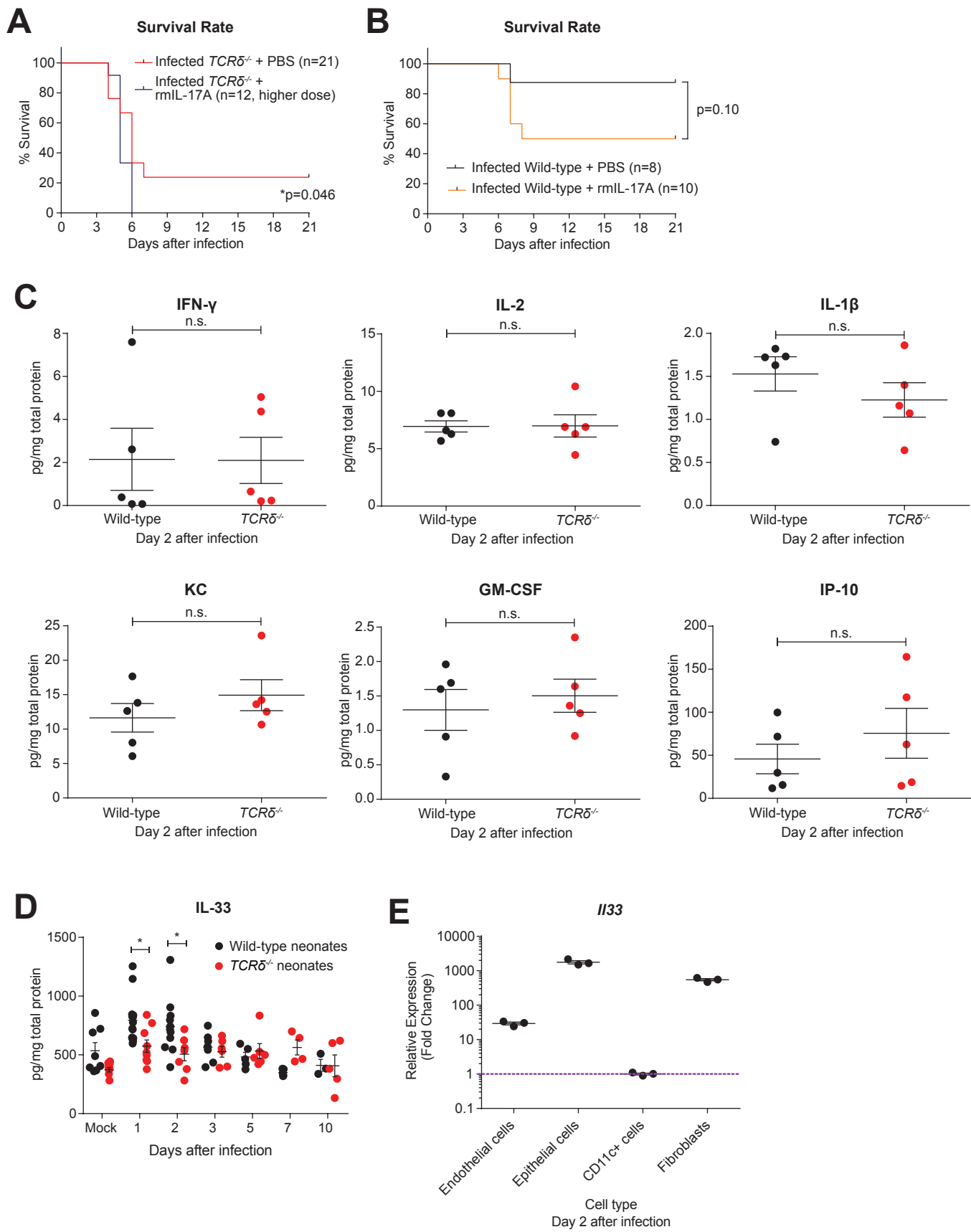


Figure S4

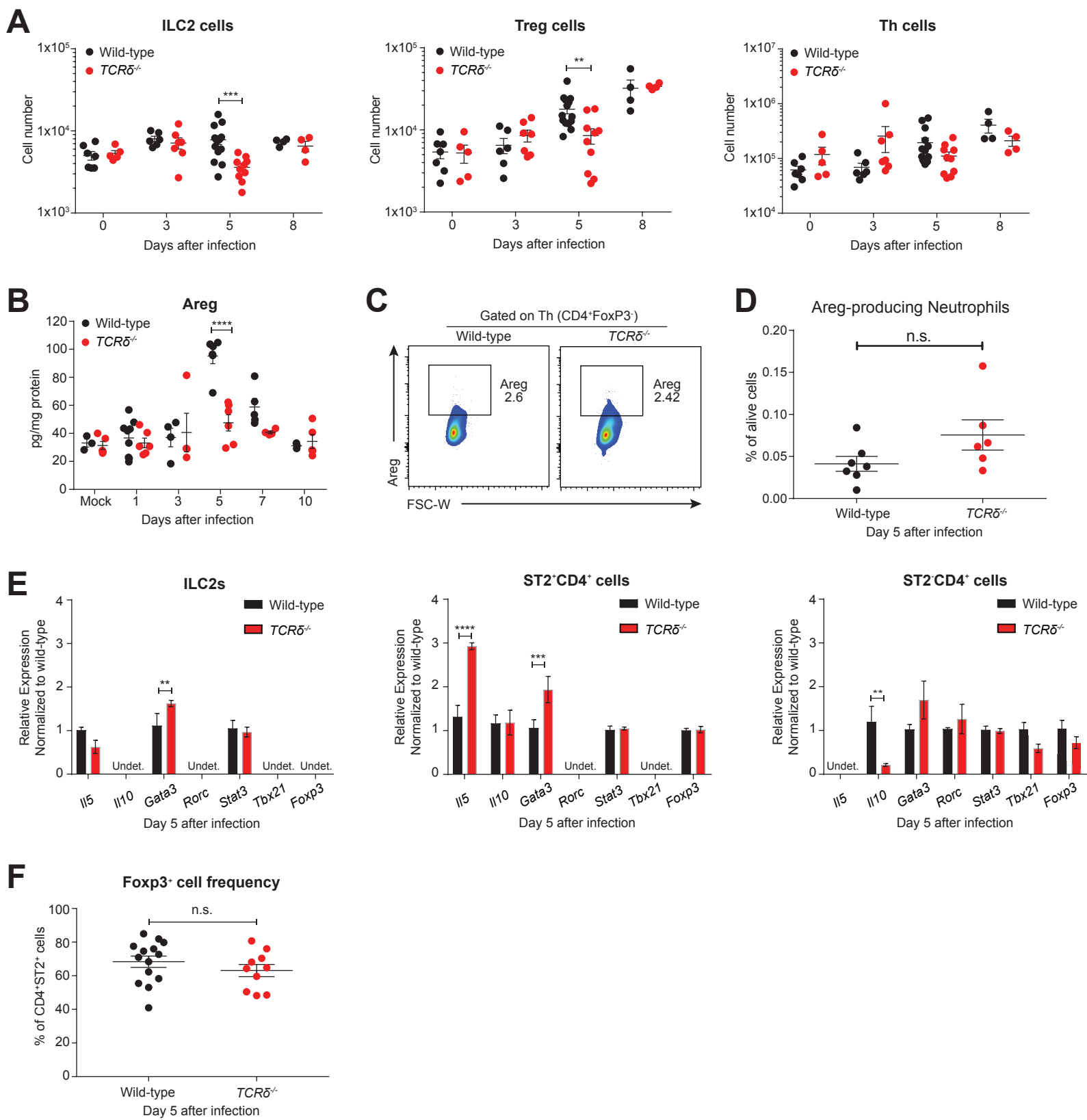


Figure S5

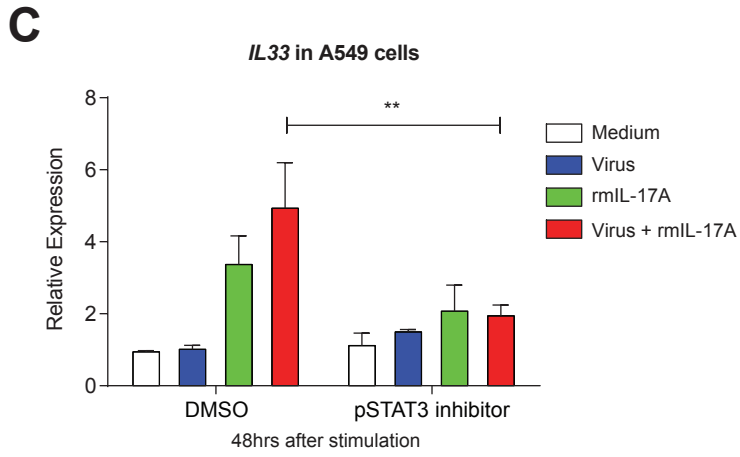
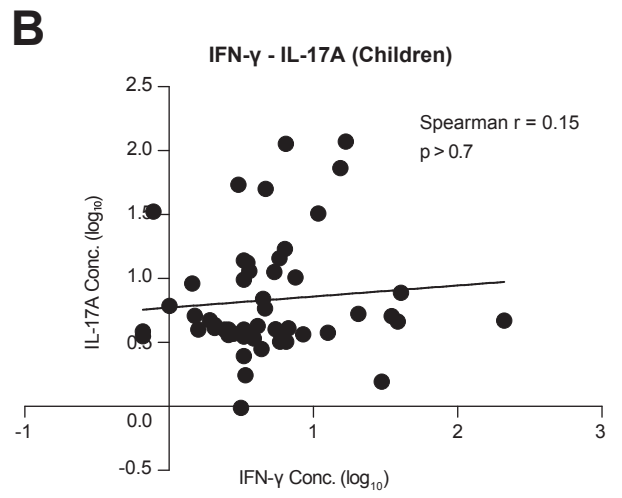
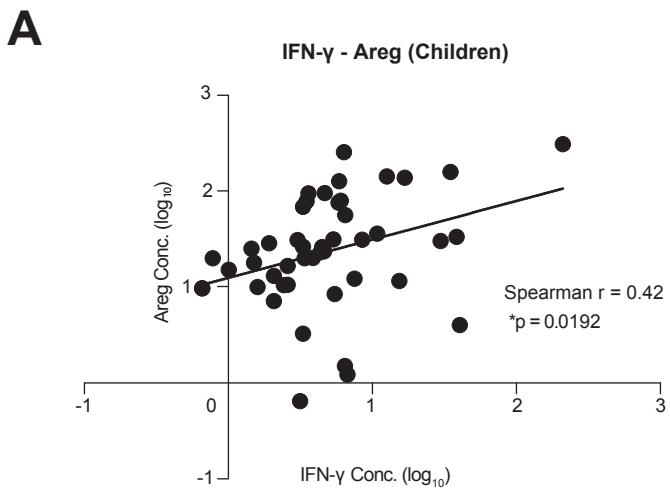


Figure S6

Supplemental figure legends

Figure S1 Gating strategy and $\gamma\delta$ T cell prevalence in mock-infected lungs. Related to Figure 1.

- A. Schematic flow cytometric plots of the gating strategies employed during experiments.
- B. Frequency (left) and number (right) of $\gamma\delta$ T cells in the lungs of wild-type neonates at days 7, 8, and 9 after birth (equivalent to d0, d1 and d2 of mock infection). Data are combined from two independent experiments and shown as mean \pm SEM. n.s., not significant.

Figure S2 The role of $\gamma\delta$ T cells in adult influenza infection. Related to Figure 1.

- A and B. Body weight profile (A) and survival rate (B) of wild-type (black, n=15) and $TCR\delta^{-/-}$ (red, n=23) adults after virus infection, normalized to the original weight. Data are combined from four individual experiments and weight change data are shown as mean \pm SEM.
- C. Cell number of adult lung $\gamma\delta$ T cells at indicated time point after infection.
- D. Cell number of adult lung IL-17A-producing $\gamma\delta$ T cells at indicated time point after infection.
- E. Cell number of adult lung IFN- γ -producing $\gamma\delta$ T cells at indicated time point after infection.
- (C-E) Data are combined from two individual experiments with mock infection (n=7), or day 3 (n=10), day 5 (n=5), and day 8 (n=5) after influenza infection. **p<0.01.

Figure S3 Characterization of $\gamma\delta$ T cells and neutrophils in influenza-infected neonatal lungs. Related to Figure 2.

- A. Frequency (top panel) and cell number (bottom panel) of lung $\gamma\delta$ T cells (left), IL-17A-producing $\gamma\delta$ T cells (middle) and IFN- γ -producing $\gamma\delta$ T cells (right), with mock infection (n=14), or day 1 (n=11), 2 (n=10), 5 (n=13), and 8 (n=7) after infection. Data are combined from at least two individual experiments at each time point and presented as mean \pm SEM.
- B. Frequency of IL-17A-producing $\gamma\delta$ T cells in mock- (n=10) or influenza- (n=15) infected neonatal lungs at 1 day after infection, without PMA/Ionomycin stimulation. Data are combined from three individual experiments and presented as mean \pm SEM.
- C. Percent (left) and number (right) of neutrophils of wild-type or $TCR\delta^{-/-}$ neonates with influenza- infected neonatal lungs at day 0, 3, 5 and 8 following infections. Data are pooled from nine independent experiments and at least two individual experiments at each time point. Data are shown as mean \pm SEM.
- D. TRGV family usage of CD27⁺ (left) or CD27⁻ (right) $\gamma\delta$ T cells estimated by single-cell PCR at mock-infection, 2 days after influenza infection, and 6 days after influenza infection (top to bottom). TRGV sequence data in the pie chart present Mock-CD27⁺ (n=11), Mock-CD27⁻ (n=19), Day2-CD27⁺ (n=65), Day2-CD27⁻ (n=59), Day6-CD27⁺ (n=45), and Day6-CD27⁻ (n=32).
- *p<0.05, **p<0.01, ***p<0.001, ****p<0.0001, n.s., not significant. .

Figure S4 Cytokine expression and infected neonates survival with cytokine administration. Related to Figure 3.

- A. Survival rate of influenza-infected $TCR\delta^{-/-}$ neonates administered with of high-dose of recombinant mouse IL-17A (rmIL-17A, navy, 1000pg/mouse, n=12) or PBS control (red, n=21) at the time of infection. Data are combined from five independent trials that individually showed the same trend, and data are presented as mean \pm SEM.
- B. Survival rate of influenza-infected wild-type neonates administered with recombinant mouse IL-17A (rmIL-17A, orange, 100pg/mouse, n=10) or PBS control (black, n=8) at the time of infection. Data are combined from two independent trials that individually showed the same trend, and data are presented as mean \pm SEM.
- C. Protein levels of IFN- γ , IL-2, IL-1 β , KC, GM-CSF and IP-10 assessed by Milliplex assay and normalized to the total protein in the lungs of infected wild-type (black, n=5) and $TCR\delta^{-/-}$ (red, n=5) neonates at day 2 after infection. Samples are pooled from three individual experiments, and data are combined and presented as mean \pm SEM.
- D. Protein levels of IL-33 assessed by ELISA and normalized to the total protein in the lungs of infected wild-type (black) and $TCR\delta^{-/-}$ (red) neonates at indicated time points after infection. Samples are pooled from at least two independent trials at each time point, and data are presented as mean \pm SEM.

E. Relative expression results of *Il33* gene in endothelial cells, epithelial cells, CD11c⁺ cells, and lung fibroblasts isolated from neonatal lungs 2 days after infection (n=3). Data are presented as mean ± SEM.

*p<0.05, n.s., not significant.

Figure S5 Areg expression dynamics during neonatal influenza infection. Related to Figure 5.

A. Cell number of ILC2s, Treg cells, and Th cells in the lungs of wild-type (black) and *TCRδ*^{-/-} (red) influenza-infected neonates at various time point after infection. Data are combined from at least two individual experiments at each time point and shown as mean ± SEM.

B. Abundance of Areg protein was assessed by ELISA and normalized to the total protein in the lungs of wild-type (black) and *TCRδ*^{-/-} (red) influenza-infected neonates at different time points. Samples are pooled from at least two individual experiments at each time point, and data are shown as mean ± SEM.

C. Representative flow cytometric plots of Areg-producing Th cells in wild-type and *TCRδ*^{-/-} lungs at day 5 following infection.

D. Frequency of Areg-producing neutrophils in influenza-infected wild-type (n=7) and *TCRδ*^{-/-} (n=6) lungs at day 5 after infection. Data are combined from two individual experiments and shown as mean ± SEM.

E. Relative gene expression of *Il5*, *Il10*, *Gata3*, *Rorc*, *Stat3*, *Tbx21* and *Foxp3* in ILC2s, ST2⁺CD4⁺ cells and ST2⁻CD4⁺ cells sorted from wild-type (n=5) and *TCRδ*^{-/-} (n=5) lungs at day 5 after infection. Samples are pooled from two independent experiments and data are presented as mean ± SEM.

p<0.01, *p<0.001, ****p<0.0001, n.s., not significant.

Figure S6 Correlation of IFN-γ - Areg and IFN-γ - IL-17A in children, and *IL33* gene expression in stimulated A549 cells. Related to Figure 6.

A. Correlation between concentration of human IFN-γ (x-axis) and Areg (y-axis) in influenza-infected children (n=51). Cytokine values (pg/ml) were log₁₀ transformed for visualization.

B. Correlation between concentration of human IFN-γ (x-axis) and IL-17A (y-axis) in influenza-infected children (n=51). Cytokine values (pg/ml) were log₁₀ transformed for visualization.

C. Relative expression of *IL33* transcripts in human lung epithelial cells (A549) treated with DMSO or the pSTAT3 inhibitor and stimulated for 48 hours with medium, influenza virus, rmIL-17A, or the virus-rmIL-17A combination. Data are shown as mean ± SEM and combined from three separate experiments that independently showed the same trend. *p<0.05, **p<0.01.

Table S1 Primers for mouse $\gamma\delta$ TCR sequencing. Related to STAR Methods - Single-cell Sorting and Multiplex PCR.

Primer name	External	Internal
TRGV1-3For	GCAGCTGGAGCAAACCTG	CTGAATTATCGGTCACCAG
TRGV4For	CAAATATCCTGTAAAGTTTTCA TC	GTTTAGAGTTTCTATTATATGTCCTTGC AAC
TRGV5For	GATATCTCAGGATCAGCTCTC C	TACCCGAAGACCAAACAAGAC
TRGV6For	TCACCTCTGGGGTCATATG	AGAGGAAAGGAAATACGGC
TRGV7For	CAACTTGGAAGAAAGAATAAT GTC	CACCAAGCTAGAGGGGTC
TRGCRov	CTTTTCTTTCCAATACACCC	TCDGGAAAGAACTTTTCAAGG